INFLUENCE OF CREEP AND STRESS STATES ON ALKALI-SILICA REACTION INDUCED-EXPANSION OF CONCRETE UNDER RESTRAINT

Yuichiro Kawabata[1, 2*], Jean-François Seignol[1], Renaud-Pierre Martin[1], François Toutlemonde[1],

[1] Université Paris-Est, IFSTTAR, Materials and Structures Department, Marne-la-Vallée, FRANCE

[2] Port and Airport Research Institute, Structural Engineering Division, Yokosuka, JAPAN

Abstract

Creep and applied stress states or restraints have a significant influence on deformation of reinforced concrete structures affected by alkali-silica reaction (ASR). This influence may also be important when a structure subjected to ASR is submitted for retrofitting/mitigation purposes to additional compression provided by jacketing or pre-stressing. It still remains controversial, however, how the combination of creep and stress states or restraints affect the expansion behaviour of concrete induced by ASR. This paper describes the model proposed to account for the influence of creep and stress states on the expansion of concrete induced by ASR on the basis of chemo-visco-elasticity. Experimental results of the literature were compared to calculated ones which can be obtained by the proposed macroscopic model. The results emphasized a necessity to take creep and damage into account for numerical re-assessment of ASR-affected concrete.

Keywords: alkali-silica reaction, creep, model anisotropy, damage

1 INTRODUCTION

The structures affected by Alkali-Silica Reaction (ASR) to be re-assessed are frequently subjected to permanent loads such as dead weight, permanent external loadings or pre-stressing. Stresses make the strain variations within the structures rather complex to be analyzed. Steel reinforcement in concrete also restrains the expansion of concrete which can make the problem even more complicated [1-2]. In highly stressed or restrained concrete, ASR-induced expansion shows strong anisotropic behavior [2-8]. In concrete subjected to stresses or restraint, creep plays an important role in the delayed deformation of ASR-affected structures. This may also have a significant influence when an ASR-affected structure is submitted to external pre-stressing or jacketing for mitigating ASR effects. The complex combination of ASR and creep therefore shall deserve refined modeling. Though some numerical approaches have been developed, it is not clear how to model and implement creep in the numerical analysis.

In this paper, therefore, the previous literature references have been summarized briefly, focusing on the experimental facts and numerical approaches regarding interaction between creep, damage and ASR expansion. Then this paper describes the macroscopic model on the basis of chemo-visco-elastic approach to take into account the influence of creep on the expansive behavior of concrete subjected to compression and restraint. The validation of the model by comparison with available experiments is carried out.

2 LITERATURE REVIEW

2.1 Experimental evidence

There have been numerous experiments for uni-axially compressed/restrained concrete members whilst expansion data under multi-axial restraint is still lacking. The exhaustive experiments by Multon and Toutlemonde [3] revealed that volumetric expansion imposed by ASR is almost constant whatever the stress conditions for the aggregate they used. They also reported that expansion can transfer to less-compressed direction, resulting in strong anisotropic expansion. This is called as "expansion transfer effect" and has been confirmed by many experiments: restraint by steel bars embedded in concrete [5]; restraint by steel rods installed externally [6]. Dunant and Scrivener, however, claimed that the microstructural situation is more complicated, from expansion test under

* Correspondence to: kawabata-y@pari.go.jp

uni-axial stresses (0, 5, 10 and 15 MPa) and numerical simulation [9]. They observed experimentally that the volumetric variations above 10 MPa are only derived from lateral expansion and no expansion for longitudinal direction. The numerical simulation showed an orientation of cracks which changes expansive behaviour. According to the experiments by Berra et al., expansion transfer effect may depend on the type of reactive aggregate [10].

In the previous experimental studies, the creep strains are subtracted from the measured strains with an assumption that the instantaneous and creep strains of ASR-reactive concrete are the same as those of non-reactive concrete. The experimental evidence, however, shows that mechanical properties are also degraded due to ASR expansion. The previous experimental results regarding the relationship between expansion and the reduction ratio of Young's modulus are summarized in Figure 1 (a) [1, 8, 11-15]. The reduction ratio of Young's modulus is normalized by using Young's modulus of non-reactive concrete. Figure 1(b) and (c) show the ASR-induced reduction of tensile strength and compressive strength [11]. It is clear from this reference as well as a number of other programs that Young's modulus and tensile strength are strongly influenced by ASR expansion. Compressive strength is less sensitive to ASR expansion but it may be reduced up to 20 % at the expansion of 0.3%. These interactions should be taken into account when interpreting the experimental results.

2.2 Numerical analysis

Some numerical tools have been developed to cope with re-assessment of the structures affected by ASR [11, 16-21]. Using these tools is a promising way to solve the complicated coupled problem. Regarding how to model and implement creep in the analysis, different approaches have been performed by different numerical tools. In the model by Saouma et al. [17], the effective modulus was used to take into account creep effect. Multon and Toutldemonde [3] and LMDC model [11] also adopted an effective modulus equal to one third of the instantaneous modulus at 28 days. In Lattice Discrete Particle Modeling by Alnaggar et al. [18], creep strain was modeled with macroscopic B3 model [22] and added to mesoscopically simulated results. Grimal et al. developed a rheological model to take into account creep and mechanical damage [19]. A recent microscopic approach has been developed by Giorla et al. to simulate the realistic damage in the paste by ASR expansion [23].

It still remains controversial how the combination of creep and stress states or restraints affects expansion and how to implement creep effect in the calculation. Especially implementation of creep in the numerical analysis depends on the global frame of mechanical calculation such as elasticity, elasto-plasticity and so on. Complicated models would be beneficial from the scientific approach, but there are many parameters to be calibrated so that applicability of the model to various concrete with various aggregates is not trivial. A recent paper reported that the LMDC model shows reliable applicability to various concretes with various aggregates and various water-cement ratios [11]. From the practical viewpoint, the many physical properties should be calibrated with a small number of concrete cores extracted from the affected structures, thus, models with less unknown parameters to be calibrated are recommended. Numerical analysis based on macroscopic chemo-mechanical models, in this regard, is a promising way to have as less parameters as possible. In macroscopic chemo-mechanical model, however, it has not been validated how to model and implement creep strain in the analysis. In the following chapter, therefore, the creep modelling and its implementation in the analysis on the basis of chemo-mechanical modelling is proposed.

3 MACROSCOPIC CHEMO-MECHANICAL MODELLING

This study describes the macroscopic model on the basis of chemo-mechanical approach proposed to take into account the influence of creep on the expansive behavior of concrete subjected to compression and restraint.

3.1 Chemo-visco-elasticity

On the basis of the theoretical chemo-elasticity of concrete [24, 25], total strain ε can be expressed as a sum of strains including viscous term, as in the following equation (1).

$$\varepsilon = \varepsilon_e + \varepsilon_\chi + \varepsilon_{cr} + \varepsilon_{sh} \tag{1}$$

in which the concrete total strain tensor ε is sum of four strains: elastic strain ε_e; ASR-induced chemical strain ε_χ; creep strain ε_{cr}; shrinkage strain ε_{sh}. Elastic strain relates to stress tensor by Hooke's law:

$$\underline{\sigma} = (K - 2/3 \times G)\, tr\, \underline{\underline{\varepsilon}}_e \underline{\underline{I}} + 2G \underline{\underline{\varepsilon}}_e \tag{2}$$

where K and G are, respectively, the bulk modulus:

$$K = E / 3(1-2\nu) \tag{3}$$

and the shear modulus:

$$G = E / 2(1+\nu) \tag{4}$$

where E is the Young's modulus and ν is the Poisson's ratio of the material.
Assuming that ASR and creep strains are prescribed strains, stresses and strains can be calculated with equation (2).
The details for mathematical models for ASR expansion and creep are described in the following.

3.2 ASR expansion

According to the references [24, 25], ASR-induced expansion can be formulated as the product of potential swelling ε_∞ and chemical advancement function of time $\xi(t)$, see equation (5).

$$\varepsilon_\chi = \varepsilon_\infty \xi(t) \tag{5}$$

This kinetic function represents the degree of reaction which evolves from 0, at the beginning of reaction, to 1, at the end of reaction and it can be described with two parameters as in the following equation (6).

$$\xi(t) = \{1 - \exp(-t/\tau_C)\} / \{1 + \exp(-(t - \tau_L)/\tau_C)\} \tag{6}$$

where, t is elapsed time, τ_C and τ_L are characteristic time and latency time, respectively (for the schematic image, see Figure 2).

It has been sometimes observed that the expansion along the vertical direction (parallel to casting direction) is much larger than that of horizontal direction, when expansion tests on cylinder concrete specimens have been performed [26]. This intrinsic anisotropy is due to preferential orientation of microcracks and interfacial transition zone perpendicular to casting direction, resulting in larger expansion in the vertical direction. An intrinsic anisotropy coefficient a_i can be expressed as the ratio of horizontal expansion ε_h to vertical expansion ε_v, (where the vertical direction is the casting direction) which can be written:

$$a_i = \varepsilon_h / \varepsilon_v \leq 1 \tag{7}$$

According to the previous experiments and field experience [27], a_i ranges from 0.6 to 1, depending on the type of aggregate and/or concrete mix and casting conditions. Therefore, free expansive strain tensor induced by ASR without restraint can be defined as [16]:

$$\varepsilon_\chi(t) = \varepsilon_\infty \xi(t) A_i \tag{8}$$

where, A_i is the intrinsic anisotropy tensor which can be written:

$$A_i = \begin{pmatrix} a_i & 0 & 0 \\ 0 & a_i & 0 \\ 0 & 0 & 1 \end{pmatrix} \tag{9}$$

in a frame where third coordinate corresponds to gravity direction during casting.
The stress state also strongly influences anisotropic ASR expansion. According to Seignol et al. [16], the stress-induced anisotropy for ASR expansion can be defined as:

$$\varepsilon_\chi(\sigma) = A_s(\sigma)\, \varepsilon_\chi(0) \tag{10}$$

where, the anisotropy tensor A_s is

$$A_s = \begin{pmatrix} \cos^2 a \cos^2 \beta & 0 & 0 \\ 0 & \cos^2 a \sin^2 \beta & 0 \\ 0 & 0 & \sin^2 a \end{pmatrix} \quad \text{in the frame of principal stresses.} \tag{11}$$

The two parameters, a and β, are defined by

$$2\tan^2 a = \frac{f_{ct}^2(1-\nu)}{(S_3 - f_{ct})^2} + \nu \tag{12}$$

$$\tan^2 \beta = \frac{f_{ct}^2(1-\nu)}{\left((S_2 - S_1)/2 - f_{ct}\right)^2} + \nu \tag{13}$$

where, S_1, S_2 and S_3 represent the stress deviator eigenvalues, f_{ct} is the tensile strength of concrete and ν is Poisson's ratio.

3.3 Creep

As long as stresses remain lower than 40% of compressive strength f_c', creep strain can be assumed to be linearly related to the applied stress and the principle of superposition is valid [28]. When concrete is subjected to a constant stress σ_{appl} applied at time t_0, creep strain ε_{cr} at time t can be written:

$$\varepsilon_{cr} = \frac{\sigma_{appl}}{E} \phi(t; t_0; T; h) \tag{14}$$

where, E is Young's modulus and creep coefficient of concrete ϕ is defined as [29]:

$$\phi(t; t_0; T; h) = h \frac{T-25}{45} \frac{k_{fp}}{\sqrt{f_c}} \frac{\sqrt{t-t_0}}{b + \sqrt{t-t_0}} \tag{15}$$

where h is saturation grade, T is temperature (expressed in Kelvin) and k_{fp} and b are material parameters.
This model derives from Granger's works [30] and usual shape of creep kinetics in French and European design codes [28].

3.4 Damage

Advancement of ASR induces microcracks of concrete, resulting in degradation of mechanical properties. Especially, ASR-induced microcracking strongly affects Young's modulus which should be taken into account. The ASR-induced damage d can be defined as [16, 31]:

$$d = d_{max} \left(1 - \exp\left(- \omega \langle \varepsilon_\chi - \varepsilon_0 \rangle^+\right)\right) \tag{16}$$

where, ε_0 is the expansion above which cracking starts in the aggregate or paste, d_{max} and ω are materials parameters representing maximum damage and rate of damage evolution (calibrated on laboratory tests), respectively; $\langle x \rangle^+$ denotes the positive part of x.
Therefore degraded Young's modulus E can be described according to equation (17).

$$E = E_0 (1-d) \tag{17}$$

where, E_0 is the undamaged Young's modulus. Note that this damaged module also modified equation (14), which represents the variation of creep properties induced by ASR.

4 SIMULATIONS OF THE PREVIOUS EXPERIMENTS

In this section, the experimental data by Multon and Toutlemonde [3] were utilized to validate the model proposed in the former section. The calculated results were compared to the experimental results.

4.1 Methods for assessment and analysis

The experimental results of Multon and Toutlemonde [3] were utilized for analysis (Figure 3(a)). Expansion tests were performed on cylinder specimens (130 mm in diameter, 240 mm height) under multi-axial restraint, with different applied axial stress (0 and 10MPa) and thickness of circumferential steel rings (no ring, 3 mm and 5 mm) for passive restraint. The concrete specimens were cured at room temperature for 28 days and then stored at 38 °C. Then the axial stresses were applied on the concrete specimens. The radial deformation was restrained by steel rings while the axial restraint by these steel rings could be neglected since each steel ring was independent from the others. Axial and radial deformations of the specimens were monitored up to about 450 days by automated measurement device. The concrete specimens were also kept sealed with watertight cover in order to obtain a homogeneous moisture state and resulting homogeneous ASR expansion. The creep of non-reactive concrete under applied stress was also measured.

The calculations were performed to simulate the experiments of concrete with/without steel rings under 0 to 10 MPa of applied vertical stress. The mechanical properties of reactive and non-reactive concretes were almost the same so that the creep material parameters b and k_{fp} of reactive concrete were assumed to be identical as for non-reactive concrete, and so was shrinkage. In fact, Young's modulus of reactive and non-reactive concrete was 37.3 GPa and 37.2 GPa, respectively [1].

Because of the cylindrical symmetry of the specimens, orthoradial strains in concrete are the same as radial ones. The boundary conditions for calculations are as follows: (1) the axial stress at the ends of the specimens is equal to the applied stress; (2) The radial displacements at the interface between concrete and steel ring are the same; (3) The radial stress on the external steel ring surface is zero; (4) The confinement effort applied by the steel rings on the concrete equals the pressure of the concrete on the steel rings.

In order to evaluate the effect of features of the model described above, 3 different simulations were performed for each experiment, leading to three cases. In Case 1, the whole model was used. In Case 2, couplings of ASR expansion and creep have been implemented to evaluate the effect of creep on concrete deformation including ASR expansion, but damage (Eqs. (16) - (17)) was not taken into account. Case 3 deals with modification of mechanical properties by ASR expansion whereas creep (Eqs. (14) - (15)) is not taken into account.

4.2 Algorithm for calculation

Based on the model described in the former section, the visco-elastic response under applied load and chemical expansion induced by ASR is integrated in the calculation system. The calculation system was set up in an Excel calculation sheet, as a simplified tool, with respect to the numerical analysis software RGIB which has been developed by Ifsttar [16]. The algorithm for calculation is shown in Figure 3(b). At time t after applying compressive stress or restraint, using the stress and displacement fields computed from the previous timestep, increments of prescribed creep and chemical strains during time step (Δt) can be calculated. Regarding ASR-induced chemical strain, anisotropic chemical strain based on stress-induced anisotropy is calculated. Mechanical calculation including prescribed strains (Eq. (2)) resolves the modified stress fields and displacement fields. These updated stress and displacement fields are utilized for the next time step $t + \Delta t$. Chemical strain also leads to damage of concrete so that the modified mechanical properties are also updated. Damaged mechanical properties modify visco-elastic strains and anisotropy coefficient. After calculation, the advancement calculation at $t + \Delta t$ is performed. The calculation was looped over time up to 500 days. The timestep was 0.1 day up to 7 days after loading and then was increased to 1 day up to 500 days.

4.3 Parameter identification

The parameters for creep were calibrated with the data of non-reactive concrete with applied stress. The experimental data of unloaded non-reactive concrete were directly used for shrinkage model. For damage model, experimental data and model are plotted in Figure 1. ε_0, d_{max} and ω have been calibrated with the least square method as 0.02 %, 0.7 and 6, respectively. ASR expansion was calibrated by subtracting shrinkage strain of non-reactive unloaded concrete specimens from the measured strain of unloaded reactive concrete specimens (Figure 4), leading to τ_C = 75 days, τ_L =126 days, ε_∞ =0.115 % and a_i=0.75.

4.4 Results

The expansive behaviour of concrete restrained by steel rings (3 mm & 5 mm) is shown in Figure 5 (a) and (b), respectively. In the figure, positive values indicate expansions and negative values contractions. Under restraint without vertical stress, all the calculations are similar: they slightly

overestimate the experimental results in the axial direction. With steel restraint along radial direction (3 and 5-mm-thick rings), the horizontal expansion is transferred to the free direction, resulting in larger expansions along the vertical axis. The results given by the model caught general trends similar to the experimental ones. According to the stress evolution in steel rings as predicted with Case 1 calculation, the maximum restraint stress induced by steel ring was 2.6 ± 0.2 MPa for 3 mm rings and 3.0 ± 0.2 MPa for 5 mm rings, respectively: they are close to simplified simulation with delayed Young's modulus [1].

Experimental and calculated results for concrete samples without steel rings subjected to vertical stress of 10 MPa are shown in Figure 6. For transversal strain, all the calculations showed almost the same tendencies: they overestimated the experimental result. Regarding vertical strain, each case was significantly different; Case 3 calculation was quite far from the experiments which emphasizes the need to take creep into account. Case 1 and Case 2 showed similar trends up to 100 days. At 500 days, however, the absolute difference between them reached 0.026 %. This is because the damage due to ASR modifies mechanical properties of concrete, resulting in larger creep and elastic strains. Finally, concerning vertical direction, Case 1 fairly agreed with the experiment, even though the calculation underestimated the experiments. It turned out to be necessary that stress-induced anisotropy should be implemented in the calculation to have the consistent result.

Figure 7 (a) and (b) show the experimental and numerical results for the samples with steel rings (3 mm & 5 mm respectively) and subjected to vertical stress of 10 MPa. Once again, the Case 3 calculation showed noticeable discrepancies with the experiments. Case 1, on the contrary, fairly simulated the experimental behavior in vertical direction for both restraint conditions. Case 2 calculations were also close to the experimental results. Regarding the results in the radial direction, the difference between various models was hardly distinguished whilst all the calculations showed larger expansion than the experiments.

5 DISCUSSION

The results shown above emphasize the need to take creep into account for numerical assessment of ASR-affected concrete structures, especially for highly compressed concrete which shows strong anisotropic expansion. On the basis of chemo-visco-elasticity, the assumption of incremental strain-model for implementation of both creep and ASR-induced expansion is successfully validated by comparison with the experimental results. Creep has a significant role to modify deformation of concrete which should be taken into account for assessment of the structures affected by ASR.

The analytical results also suggest a necessity to implement damage in the calculation which changes mechanical properties and results in visco-elastic response of concrete affected. In this study, though the simplified isotropic damage model was identified by using the previous experimental data, the results were more consistent with the experiments. More refined models such as anisotropic damage model [32] would be necessary for further research.

Further validation will be carried out for other experimental data such as large-scale beams tested by Multon et al. [4].

6 CONCLUSIONS

A creep model was implemented in the chemo-mechanical calculation of ASR-affected concrete with the assumption that creep strain is an additive strain as well as ASR-induced chemical strain. The simulation turned out well consistent with the experiments, which supports the assumptions described above. It was strongly confirmed that creep has an important role to modify the deformation of concrete so that it is necessary to implement it in the calculation. Damage model is also necessary to be implemented to give more consistent results.

7 REFERENCES

[1] S. Multon, Evaluation expérimentale et théorique des effets mécaniques de l'alcali-réaction sur des structures modèles, Université de Marne la Vallée, 2003 (in French).

[2] N. Smaoui, Contribution à l'évaluation du comportement structural des ouvrages d'art affectés de réaction alcali-silice (RAS), Ph.D. thesis, Université de Laval, 2003 (in French).

[3] S. Multon and F. Toutlemonde, Effect of applied stresses on alkali-silica reaction-induced expansion, Cement and Concrete Research, 35 (2006) 912-920.

[4] S. Multon, J. -F. Seignol and F. Toutlemonde, Structural behavior of concrete beams affected by alkali-silica reaction, ACI Materials Journal, 102 (2003) 67-76.

[5] T. U. Mohammed, H. Hamada and T. Yamaji, Relation between strain on surface and strain over embedded steel bars in ASR affected concrete members, Journal of Advanced Concrete Technology, 1 (2003) 76-88.
[6] H. Kagimoto, Y. Yasuda and M. Kawamura, ASR expansion, expansive pressure and cracking in concrete prisms under various degrees of restraint, Cement and Concrete Research, 59 (2014) 1-15.
[7] L. Charpin and A. Ehrlacher, Microporomechanics study of anisotropy of ASR under loading, Cement and Concrete Research, 63 (2014) 143-157.
[8] C. Larive, Apports Combinés de l'Expérimentation et de la Modélisation à la Compréhension de l'Alcali Réaction et de ses Effects Mécaniques, Laboratoire Central des Ponts et Chaussées (1998) (in French).
[9] C. F. Dunant and K. Scrivener, Effects of uniaxial stress on alkali-silica reaction induced expansion of concrete, Cement and Concrete Research, 42 (2012) 567-576.
[10] M. Berra, G. Faggiani, T. Mangialardi and A. E. Paolini, Influence of stress restraint on the expansive behaviour of concrete affected by alkali-silica reaction, Cement and Concrete Research, 40 (2010) 1403-1409.
[11] L. F. M. Sanchez, S. Multon, A. Sellier, M. Cyr, B. Fournier and M. Jolin, Comparative study of a chemo-mechanical modeling for alkali-silica reaction (ASR) with experimental evidences, Construction and Building Materials, 72 (2014) 301-315.
[12] The Institution of Structural Engineers, Structural effect of alkali-silica reaction, 1992.
[13] C. Giaccio, R. Zerbino, J. M. Ponce and O. R. Batic, Mechanical behavior of concretes damaged by alkali-silica raction, Cement and Concrete Research, 38 (2008) 993-1004.
[14] R. Pleau, M. A. Bérubé, M. Pigeon, B. Fournier, S. Raphaël, Mechanical behaviour of concrete affected by ASR, Proceedings of 8th International conference on alkali-aggregate reaction in concrete, (1989) 721-726.
[15] M. F. Habita, M. Brouxel, D. Prin, Alkali-aggregate reaction structural effects: an experimental study. 9th International conference on alkali-aggregate reaction in concrete, (1992) 403-410.
[16] J. -F. Seignol, N. Baghdadi and F. Toutlemonde, A macroscopic chemo-mechanical model aimed at re-assessment of delayed-ettringite-formation affected concrete structures, Proceedings of the 1st International Conference on Computational Techniques in Concrete Structures (2009).
[17] V. Saouma, L. Perotti and T. Shimpo, Stress analysis of concrete structures subjected to alkali-aggregate reactions, ACI Structural Journal, 104 (2007) 532-541.
[18] M. Alnaggar, G. Cusatis and G. Di Luzio, Lattice Discrete Particle Modeling (LDPM) of alkali silica reaction (ASR) deterioration of concrete structures, Cement and Concrete Composites, 41 (2013) 45-59.
[19] E. Grimal, A. Sellier, S. Multon, Y. Le Pape and E. Bourdarot, Concrete modeling for expertise of structures affected by alkali aggregate reaction, Cement and Concrete Research, 40 (2010) 502-507.
[20] C. Comi, R. Fedele, U. Perego, A chemo-thermo-damage model for the analysis of concrete dams affected by alkali-silica reaction, Mechanics of Materials, 41 (2009) 210-230.
[21] I. Comby-Peyrot, F. Bernard, P.-O. Bouchard, F. Bay and E. Garcia-Diaz, Development and validation of a 3D computational tool to describe concrete behaviour at mesoscale. Application to the alkali-silica reaction, Computational Materials Science, 46 (2009) 1163-1177.
[22] Z. Bazant and S. Baweja, Creep and shrinkage prediction model for analysis and design of concrete structures, Adam Neville Symposium: Creep and Shrinkage-Structural Design Effects, ACI-SP 194, (2000) 1-83.
[23] A. B. Giorla, K. Scrivener and C. F. Dunant, Influence of visco-elasticity on the stress development induced by alkali-silica reaction, Cement and Concrete Research, 70 (2015) 1-8.
[24] Li, K., Coussy, O. and Larive, C.: Modélisation chimico-mécanique du comportement des bétons affectés par la réaction d'alcali-silice. Expertise numérique des ouvrages d'art dégradés, Etudes et recherches des LPC, OA43, Laboratoire Central des Ponts et Chaussées, Paris (2004) (in French).
[25] F. -J. Ulm, O. Coussy, L. Kefei and C. Larive, Thermo-chemo-mechanics of ASR expansion in concrete structures, Journal of Engineering Mechanics, 126 (2000) 233-242.
[26] S. Multon, F. –X. Barin, B. Godart and F. Toutlemonde, Estimation of the residual expansion of concrete affected by alkali silica reaction, Journal of Materials in Civil Engineering, 20 (2008) 54-62.

[27] Laboratoire Central des Ponts et Chaussées: Protection et réparation des ouvrages atteints de réactions de gonflement interne du béton (2010) (in French).
[28] NF EN 1992-2, Eurocode 2- Calcul des structures en béton – Partie 2 : ponts en béton - Calcul et dispositions constructives (2006).
[29] O. Omikrine-Metalssi, J. –F. Seignol, V. –D. Le, M. Aïtsi, S. Rigobert, F. Toutlemonde and L. –I. Boldea, Integration of anisotropy, contact elements and creep in RGIB-modulus of the F. E. program "CESAR-LCPC": Application to structures affected by internal swelling reactions, Proceedings of HYDRO 2010, (2010).
[30] L. Granger, Comportement différé du béton dans les enceintes de centrales nucléaires : analyse et modélisation, Ecole Nationale des Ponts et Chaussées (1995).
[31] N. Baghdadi, Modélisation du couplage chemico-mecanique d'un béton atteint d'une réaction sulfatique interne, Ecole Nationale des Ponts et Chaussées (2008).
[32] C. Comi and U. Perego, Anisotropic damage model for concrete affected by alkali-aggregate reaction, International Journal of Damage Mechanics, 20 (2011) 598-617.

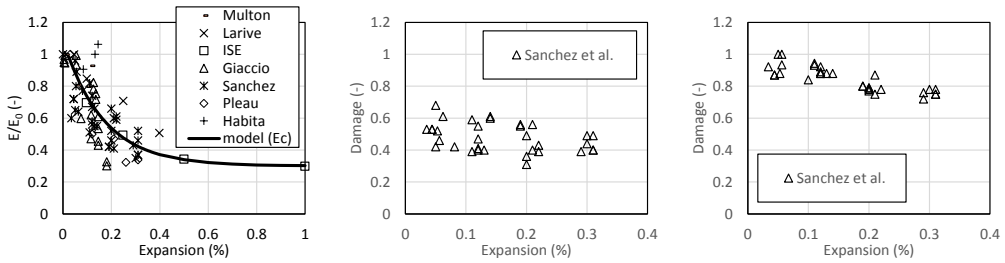

(a) Young's modulus (b) Tensile strength (c) Compressive strength

FIGURE 1: Expansion vs. mechanical properties.

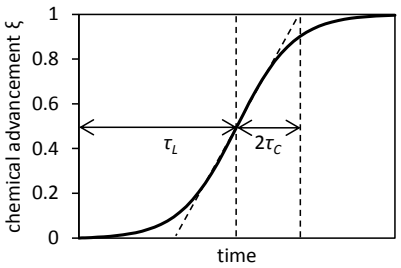

FIGURE 2: Schematic representation of chemical advancement including physical meaning of latency and characteristic times. After [7].

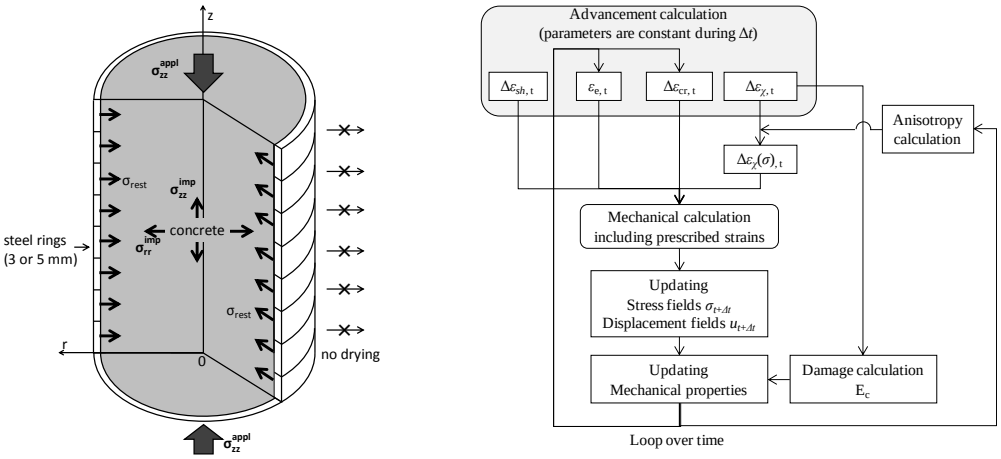

(a) Schematic image of experiments (after [2]) (b) Algorithm for calculation

FIGURE 3: Benchmarking case and calculation procedures.

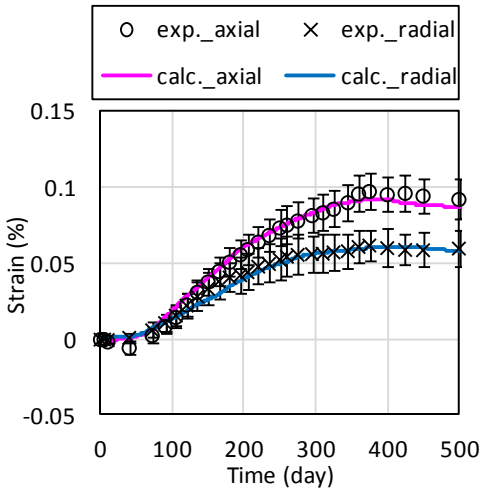

FIGURE 4: Experimental free expansion and calibrated expansion curve by the model.

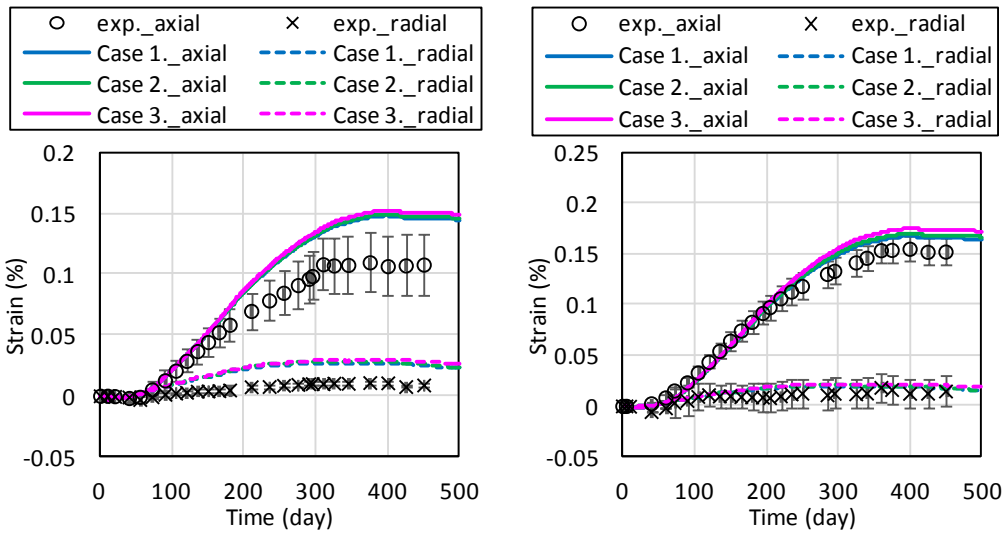

(a) 3 mm rings (b) 5 mm rings

FIGURE 5: Simulated results of concrete with steel rings (no vertical stress).

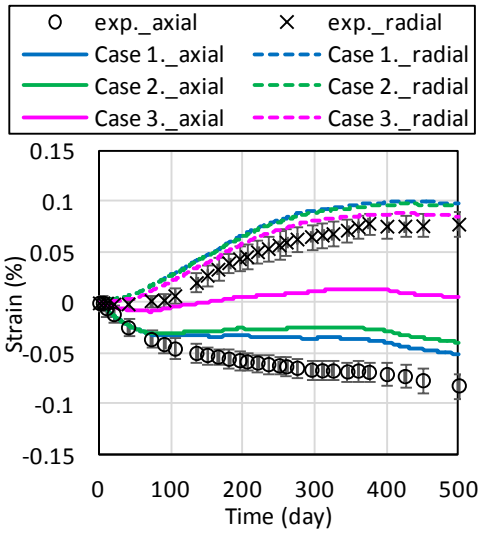

FIGURE 6: Simulated results of concrete subjected to 10 MPa (no steel rings).

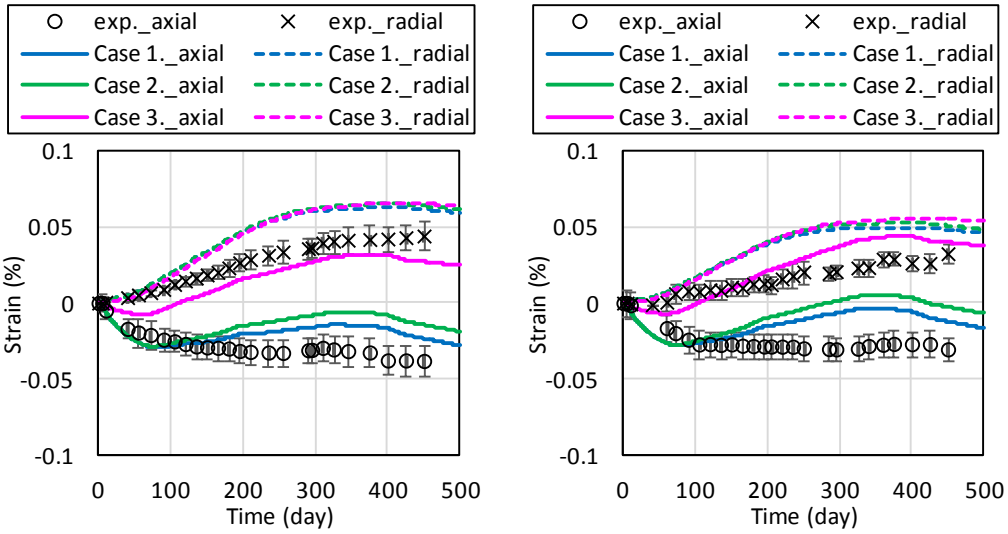

(a) 3 mm rings (b) 5 mm rings

FIGURE 7: Simulated results of concrete with steel rings and vertical stress of 10 MPa.